ELSEVIER

Age-related functional reorganization, structural changes, and preserved cognition

David Meunier [a,1], Emmanuel A. Stamatakis [a,b], Lorraine K. Tyler [a,*]

[a] Centre for Speech, Language and the Brain, Department of Psychology, University of Cambridge, Cambridge, UK
[b] Division of Anaesthesia, School of Clinical Medicine, University of Cambridge, Addenbrooke's Hospital, Cambridge, UK

ABSTRACT

Although healthy aging is associated with general cognitive decline, there is considerable variability in the extent to which cognitive functions decline or are preserved. Preserved cognitive function in the context of age-related neuroanatomical and functional changes, has been attributed to compensatory mechanisms. However, the existing sparse evidence is largely focused on functions associated with the frontal cortex, leaving open the question of how wider age-related brain changes relate to compensation. We evaluated relationships between age-related neural and functional changes in the context of preserved cognitive function by combining measures of structure, function, and cognitive performance during spoken language comprehension using a paradigm that does not involve an explicit task. We used a graph theoretical approach to derive cognitive activation-related functional magnetic resonance imaging networks. Correlating network properties with age, neuroanatomical variations, and behavioral data, we found that decreased gray matter integrity was associated with decreased connectivity within key language regions but increased overall functional connectivity. However, this network reorganization was less efficient, suggesting that engagement of a more distributed network in aging might be triggered by reduced connectivity within specialized networks.

© 2014 The Authors. Published by Elsevier Inc.

1. Introduction

Healthy aging is typically associated with deteriorating cognitive capacities in the context of structural and functional brain changes (Craik and Salthouse, 2000; Davis et al., 2009; Pfefferbaum et al., 2000; Raz et al., 2005). However, one of the hallmarks of healthy aging is its variability, with a range of preservation and losses in structure, function, and performance across several cognitive domains. The preservation of cognitive function in some individuals and in some cognitive domains (e.g., language comprehension; Tyler et al., 2010) more than others (e.g., working memory; Salthouse, 1991) has led to the hypothesis that preserved function is underpinned by compensatory mechanisms (Cabeza et al., 2002). Because a variety of neural changes occur with aging, cognitive changes in older adults might be mediated by underlying neural changes, through processes such as dedifferentiation (Park et al., 2004) or reduced hemispheric specialization (hemispheric asymmetry reduction in older adults; Cabeza, 2002; Ghisletta and Lindenberger, 2003). These findings support the "scaffolding theory of aging and cognition"; which claims that as neural structures decline over time because of natural aging, other structures from proximal or distal brain regions are recruited to preserve function.

However, evidence for compensation requires the integration of structural, functional, and behavioral data, a combination that is rarely obtained. Moreover, studies of compensation tend to focus primarily on age-related neural changes in the prefrontal cortex, in the context of age-related performance changes in cognitive domains that usually decline with age (e.g., memory, executive function). These studies reveal increased bilateral activation (Cabeza, 2002), and increased functional connectivity (Davis et al., 2012; Yang et al., 2009) in frontal cortex with age when performance is preserved. This focus on the frontal cortex, although generating important insights, involves studies that require participants to carry out an explicit task and thus might confound age-related changes to a specific cognitive domain and to those involved in more general task-related processes. In the present study we aimed to avoid this potential problem by minimizing the influence of task-related effects by using a paradigm that does not involve an overt task.

---

* Corresponding author at: Centre for Speech, Language and the Brain, Department of Psychology, University of Cambridge, Downing Street, Cambridge CB2 3EB, UK. Tel.: +44 (0)1223 766457; fax: +44 (0)1223 766452.
  E-mail address: lktyler@csl.psychol.cam.ac.uk (L.K. Tyler).
[1] Present address: Codage et Mémoire Olfactive, Centre de Recherche en Neurosciences de Lyon, Lyon, France.

We investigated a cognitive function that tends to be preserved across the adult life span—language comprehension (Burke and Shafto, 2008; Tyler et al., 2010). Language function involves a set of bilateral neural regions including bilateral inferior frontal gyrus (IFG), superior (STG) and middle temporal gyri (MTG), angular gyrus, supramarginal gyrus, and inferior parietal lobule (Indefrey and Cutler, 2004; Price, 2012). Within this extensive system, different aspects of language processing recruit different subnetworks, with syntactic processing depending on intact left MTG (LMTG) and left IFG (LIFG) and connectivity between them (Griffiths et al., 2013; Tyler et al., 2011). In our study we focused on syntactic processing because it has the advantage of being strongly left lateralized in the young, providing the ideal basis for determining whether age-related preservation of function necessarily involves increased bilateral activity and/or connectivity.

Our main research interest was in the relationship between gray matter changes, the functional network known to be essential for preserved syntax and the wider language system. Specifically, we asked whether preservation of syntax was underpinned by changes in the neural network with which it is associated (the left fronto-temporal network) and its relationship to the wider bilateral language system. In investigating the influence of aging on hemispheric reorganization, we tested age-related hypotheses concerning the mechanisms involved, such as the dedifferentiation (Park et al., 2004), hemispheric asymmetry reduction in older adults (HAROLD; Cabeza, 2002), and scaffolding models (Park and Reuter-Lorenz, 2009).

Most studies of compensatory neural mechanisms in aging use region-specific analyses which bias toward describing local but not age-related global changes; consequently, they largely ignore the wider neural changes that take place in aging, except insofar as they are related to frontal function (Davis et al., 2008). Here we circumvent these limitations in a study that uses graph theoretic analyses to investigate the relationship between age-related changes in connectivity at local and more global levels.

Graph theoretic analysis enables the characterization of functional network properties in a unique manner not offered by other connectivity approaches. Previous attempts to characterize functional networks have mainly been carried out on resting-state functional magnetic resonance imaging (fMRI) (Ferreira and Busatto, 2013) using a variety of approaches such as machine learning (Meier et al., 2012) and seed-based functional connectivity analyses (Tomasi and Volkow, 2012). Resting-state networks have also been investigated using graph theory (Buckner et al., 2009; Bullmore and Sporns, 2009; He and Evans, 2010), but this approach has only occasionally been used with task fMRI studies (Bassett et al., 2011; Eguiluz et al., 2005; Ginestet and Simmons, 2011; Shinkareva et al., 2008). This trend is reflected in the investigation of age-related functional changes, in which most studies using graph theoretical approaches have focused on resting-state (Achard and Bullmore, 2007; Meunier et al., 2009; Wang et al., 2010) and one study examined task-related fMRI (working memory; Wang et al., 2012).

Graph theoretic analysis allows the detailed characterization of networks by examining the structural properties of graphs, where a graph is defined as a set of interactions ('connections,' or 'edges') between large numbers of areas or 'nodes' (Newman, 2003). Graph analysis provides the ideal means for studying changes in global connectivity and within local networks, and establishing relationships between neural changes and cognitive functions. Here we focus on average snapshots of brain connectivity and differences between those connectivity patterns when comparing younger with older adults responding to spoken sentences rather than the temporal evolution of connectivity in younger and older brains. We obtained functional networks using the weighted correlations

method (Dodel et al., 2005), which permits quantification of network properties at the single participant level. We used a functional connectivity index (FCI) to relate network properties with age, local and global gray matter density (GMD), and behavioral performance acquired outside the scanner.

Current hypotheses regarding age-related functional reorganization in language processing in the context of network analyses and preserved language processing performance suggest the following outcomes: (1) according to the dedifferentiation hypothesis (Ghisletta and Lindenberger, 2003), functional connectivity is expected to increase in the overall language system with aging, leading to less specialized networks for older subjects; (2) in the HAROLD model (Cabeza, 2002), it is assumed that there is reduced hemispheric specialization in aging, and thus that there will be reduced connectivity between left frontotemporal regions for language processing for the older compared with the younger group; and (3) the "scaffolding theory of aging and cognition" model, in which an increase in bilateral functional connectivity for language processing in the older compared with the young group is predicted, and is associated with changes in neural structure (Park and Reuter-Lorenz, 2009). As far as structural reorganization is concerned, it is well known that GMD decreases with age (Sowell et al., 2003), and these decreases might be associated with modulation of functional connectivity, in particular between the LIFG and LMTG (Tyler et al., 2010).

2. Methods

2.1. Participants

Forty-three healthy adult volunteers (25 female), with an age range of 19 to 75 years (mean, 43.6 years; SD, 20.3 years) gave written consent to participate in the experiment. At the time of testing, 15 volunteers were between 18 and 30 years old, 12 volunteers were between 45 and 60 years old and 16 volunteers were between 60 and 75 years old (see Table 1). The study was approved by the East of England - Essex (formerly Suffolk) Research Ethics Committee. All were right-handed native British English speakers with no history of neurological illness or head injury and were free of psychiatric illness or psychoactive medication for at least one year before scanning. No participant had audiometer measurements indicating severe hearing impairment and 42 out of 43 participants scored 28 or higher on the Mini Mental State Examination and 30/36 or higher on the Ravens progressive matrices (Raven, 1995). One participant (aged 75, the oldest participant in our sample) scored 27 on the Mini Mental State Examination. Participant demographic characteristics are shown in Table 1.

2.2. Experimental paradigm

We avoided task-related effects by asking participants to listen to spoken sentences without carrying out an explicit task (see Tyler et al., 2011 for a description of the paradigm and stimuli). The sentences, all of which were fully grammatically correct and meaningful, contained a phrase which was either unambiguous (e.g., "The teacher knew that rehearsing plays is necessary for a good

Table 1
Ages and background behavioral test scores of participants

Age range (mean, SD), y	n	MMSE mean score, SD	NART mean score, SD	Shipley vocabulary mean score, SD
18—30 (21.01, 1.56)	15	29.57, 0.65	34.67, 4.39	32.20, 2.98
45—60 (51.69, 4.75)	12	29.08, 0.90	39.50, 4.10	36.92, 2.50
60—75 (66.88, 4.41)	16	28.81, 0.83	41.13, 5.43	37.69, 2.30

Key: MMSE, Mini Mental State Examination; NART, National Adult Reading Test.

performance.") or locally syntactically ambiguous (e.g., …bullying teenagers…). The phrases were syntactically ambiguous between different syntactic roles, but it was always the case that each phrase had a strong bias (dominant interpretation) toward one interpretation ("The newspaper reported that bullying teenagers ARE a problem for the local school.") and weak bias (subordinate interpretation) toward the other ("The newspaper reported that bullying teenagers IS bad for their self-esteem."). The syntactic ambiguity can only be resolved when the listener hears the verb which immediately follows the ambiguous phrase (here 'IS' or 'ARE') and which is consistent with one interpretation or the other. Pretest data collected from an independent group of participants who did not participate in the fMRI study were used to categorize the dominant/subordinate nature of ambiguity for each sentence pair. There were 42 syntactically unambiguous sentences matched in structure to the ambiguous sentences (e.g., "The teacher knew that rehearsing plays is necessary for a good performance."). We also included 126 filler sentences which varied in syntactic structure.

Stimuli were presented in the scanner via magnetic resonance-compatible headphones, using E-Prime v.2.0 (Psychology Software Tools, Inc, Pittsburgh, PA, USA). Sentences were presented in an event-related design in a pseudorandomized order, to maximize the efficiency of the design (Josephs and Henson, 1999), during three separate sessions. There were equal numbers of items in each condition in each session, and each session lasted 12–13 minutes. To improve the detectability of response in fMRI, the interstimulus interval was jittered according to a geometric distribution with mean 3250 msec (range, 2000–7000 msec; Burock et al., 1998).

We subsequently evaluated participants' performance in follow-up testing outside the scanner. Previous studies have shown similar patterns of activity when responses are measured during passive listening and task-related fMRI (Crinion et al., 2003; Scott et al., 2000; Tyler et al., 2011; Vannest et al., 2009). Specifically, one month after scanning we obtained behavioral data from each participant on the same stimuli as used in the fMRI study, to obtain a performance measure of language processing ability. Participants listened to the sentences and pressed a response key to indicate whether the disambiguating word (IS or ARE in the examples) was an acceptable or unacceptable condition of the sentence (see Tyler et al., 2011, for details). Performance in this task measures sensitivity to syntactic information during the processing of a spoken sentence. The subordinate sentences are frequently deemed to be unacceptable to young, healthy participants indicating their sensitivity to a local, and temporary, syntactic ambiguity, which is disambiguated in a way that is inconsistent with the preferred representation that they have developed up to that point. In contrast, they consider the dominant and unambiguous sentences to be acceptable because the disambiguating word is consistent with the preferred interpretation (Tyler et al., 2011). Syntactic sensitivity for each participant was assessed as the difference between acceptability judgments for the subordinate and dominant sentences (Tyler et al., 2011).

2.3. fMRI acquisition

Participants were scanned at the MRC Cognition and Brain Sciences Unit, Cambridge, with a Siemens 3T Tim Trio MRI scanner (Siemens Medical Solutions, Camberley, UK). Functional images comprised 32 oblique axial slices angled away from the eyes, each 3 mm thick with an interslice gap of 0.75 mm, in-plane resolution of 3 mm, and field of view 192 mm × 192 mm. Repetition time (TR) = 2 seconds, echo time (TE) = 30 ms, and flip angle = 78°. We acquired T1-weighted structural images at 1 mm isotropic resolution in the sagittal plane, using a magnetization-prepared rapid gradient-echo sequence with TR = 2250 ms, TI = 900 ms, TE = 2.99 ms, and flip

angle = 9°. Preprocessing of the fMRI data (using SPM5 software, Wellcome Institute of Imaging Neuroscience, London, UK) comprised slice-timing correction, realignment, and spatial normalization. Movement parameters obtained at the realignment stage (translations and rotations in x, y, z directions) were included as nuisance variables in the model to account for residual movement effects. Spatial normalization used unified normalization, which combines gray matter segmentation with nonlinear warping of the image to a template in Montreal Neurological Institute space (Ashburner and Friston, 2005).

2.4. Language template

Our network analyses involved an extensive network of brain areas relevant to language processing and used parts of the Automated Anatomical Labeling (AAL) template (Tzourio-Mazoyer et al., 2002). We constructed a template informed from our own studies of language function and studies from other groups. Research in the neurobiology of language function has shown (Dronkers et al., 2004; Indefrey and Cutler, 2004) that the brain regions involved include a primarily left lateralized network which comprises left inferior frontal gyri, left STG and left MTG, left angular gyrus, left supramarginal gyrus, and left inferior parietal lobule (Indefrey and Cutler, 2004; Price, 2012). There is evidence that homologous regions in the right hemisphere (RH) are also involved for some language functions (Bozic et al., 2010; Tyler and Marslen-Wilson, 2008). Additionally, recent studies have shown that age-related neural changes can have an effect on language function, such that preserved function is underpinned by functional reorganization with greater involvement of RH regions with increasing age (Tyler et al., 2010). These reasons necessitated the inclusion of contralateral homologous regions in our language template. To summarize, the template involved 16 anatomically identified areas involved in language function—bilateral inferior frontal gyri (triangularis, opercularis, and orbitalis, labeled IFGtriang, IFGoperc, and ORBinf, respectively), bilateral inferior, middle, and superior temporal gyri (labeled ITG, MTG, and STG, respectively), bilateral angular gyri and bilateral superior aspect of the temporal pole (labeled ANG and TPOsup, respectively).

To minimize artifactual correlations between neighboring voxels and maximize the number of voxels included in the analysis (Zalesky et al., 2010) we divided each AAL area into smaller cubical regions of interest (ROIs). These cubes consisted of $4 \times 4 \times 4$ voxels (each voxel the dimension of $2 \times 2 \times 2$ mm^3), with an inclusion criterion of at least 80% of voxels in an AAL region. To exclude ROIs on the edge of the brain, which may have introduced background (not brain) signal in the analyses, we applied an additional criterion which dictated that at least 50% of voxels in each cubical ROI had a blood oxygen level-dependent signal that was >50 in all of the volunteers scans (Fornito et al., 2010). The value of 50 is empirical and we obtained it by plotting histograms of echo-planar imaging (EPI) intensities for all subjects (see Supplementary Fig. 1). This process resulted in a network of 166 nodes. All of the analyses reported herein involve data extracted from the language template (see Fig. 1).

2.5. FCI

To obtain a measure of each participant's functional connectivity between each pair of ROIs, time series were extracted using MarsBaR (available at http://marsbar.sourceforge.net/), movement parameters were regressed, and resulting signals were filtered (band-pass: 0.005 Hz, 0.1 Hz) and normalized (z score) for each session separately. To estimate cognitive activation-dependent functional connectivity for each sentence, we used the weighted
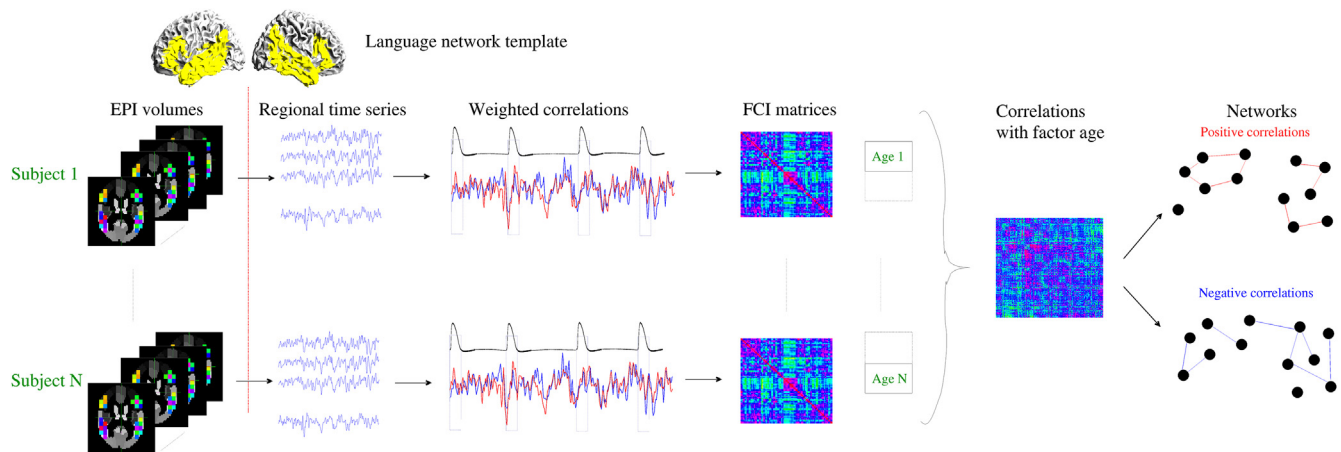
Fig. 1. Weighted correlation method. Time series are extracted for each region of interest (ROI) defined in the language network template by weighting correlation contribution according to the expected temporal course of the task convolved with hemodynamic function. The language network template shows the mask obtained by concatenating Automated Anatomical Labeling regions involved in language processing (see main text). The different ROIs are displayed on the EPI volumes as cubes of different colors. Correlations between pairs of time series are then computed, by weighting correlation contribution according to the expected temporal course of the task convolved with hemodynamic function. Gathering FCI values obtained for all pairs of ROIs results in an FCI matrix. The FCI values obtained for each pair of areas are then correlated across participants with an external factor, for example, age. The significant correlations are then sorted according to the signs, and displayed as edges on a network. Abbreviations: EPI, echo-planar imaging; FCI, functional connectivity index.

correlations method (Dodel et al., 2005). The method involves computing correlations between time points for two time series extracted from each pair of ROIs, and weighting the contribution of each pair of time points to the correlation by the condition-based regressor (Fig. 1). The weighting of the contributions of the time series to the correlation by the expected shape of the experimental task allows one to model networks that are related to a given experimental condition. As discussed in Dodel et al. (2005), the weighted correlation method leads to results comparable with those obtained with psychophysiological interaction (Friston et al., 1997), except that this method allows the investigation of synchronous interactions between multiple areas.

A measure of functional association was obtained for all ROI pairs, using the weighted correlation method. We refer to values obtained as FCI, and obtain an FCI matrix for each participant by condition. Global FCI refers to the average FCI absolute values across all values in the matrix (matrix diagonal excluded), and allows us to quantify variation in FCI at the global level within the entire bilateral language template. Negative correlation values were treated like positive values, but proved to be very rare in the dataset.

2.6. GMD

Previous studies have shown that correlations between continuous measures of neural tissue integrity (in gray and white matter) and continuous measures of behavioral performance are remarkably sensitive to brain–behavior relationships (Bright et al., 2008; Taylor et al., 2009; Tyler et al., 2005). We applied this method to the current dataset to investigate structure–function relationships by correlating FCI (see previous section) and GMD. Normalized T1 structural images were used to compute gray matter segments for each participant. The gray matter images were used to extract GMD data for each ROI in the language template. We used unmodulated images, and preserved local gray matter concentrations. For completeness we show in Supplementary Fig. 2 that the correlation between unmodulated and modulated gray matter values is highly significant. Eleven of the 166 ROIs extracted from the AAL template were outside the structural images in more than 50% of the participants and were not included in the analysis. The calculation of global GMD involved averaging the GMD extracted for all ROIs used in the language template and was used as a proxy for

assessing overall structural density of the language system. Pearson correlation coefficients were computed between GMD in a given ROI and FCI between this ROI and all other ROIs.

2.7. Network efficiency

Network efficiency is the measure we used to assess the quality of information transfer within a graph (Achard and Bullmore, 2007; Latora and Marchiori, 2001). The definition of efficiency in a binary (unweighted) graph is based on the length of shortest paths between all pairs of nodes. For a binary graph G with N, the global efficiency $E_{glob}(G)$ is defined as the sum of the inverse of the shortest paths between all pairs of nodes in the network:

$$E_{glob}(G) = \frac{1}{N(N-1)} \sum_{i \in G, \, j \in G, \, i \neq j} \frac{1}{d_{ij}}$$

with d_{ij} the length of the shortest path between node i and node j.

Efficiency was initially defined for binary (unweighted) graphs (Latora and Marchiori, 2001), and later extended to weighted graphs (Latora and Marchiori, 2003). However, for fully connected weighted graphs (i.e., when a non-zero value exists for all the pairs in the graph, as is the case for correlation-based networks), the results on efficiency do not hold (Ginestet et al., 2011). A better method in that case is to compute efficiency by thresholding the weighted graph W, leading to a binary graph G_d with density d, and to integrate the values of efficiency over the range of densities (Ginestet et al., 2011):

$$IE_{glob}(W) = \int_{d \in [0,1]} E_{glob}(G_d)$$

This measure is referred to as "integrated global efficiency," and eliminates subjective choice of a given value of threshold (Ginestet et al., 2011).

2.8. Statistical analysis

Behavioral results on acceptability judgment were analyzed using an analysis of variance, with age and syntactic conditions as factors. We used linear regressions to investigate the influence of

age and global GMD on average FCI. Overlap correlation (Meng et al., 1992; Steiger, 1980) allows the quantification of the possible relationship between correlation of Y and X1 and correlation of Y and X2, taking into account the fact that X1 and X2 are correlated, and were used to assess differences between the correlation of FCI and age and correlation between average FCI and global GMD.

To study FCI matrices at the pairwise level, we adopted the statistical parametric network framework proposed by Ginestet and Simmons (2011), and extended it to include correlational analyses with age, behavioral performance of syntactic processing, and GMD. The statistical significance of each element in the correlation matrix can be assessed by independently testing each correlation coefficient, and then correcting for the total number of pairs in the matrix. We report false discovery rate (FDR; Hochberg, 1988)-corrected results, for $\alpha = 0.05$. Most of the significant connections at the FDR level are also significant for Bonferroni correction.

3. Results

3.1. Behavioral results

In the post-test we asked volunteers to indicate whether the disambiguating word in a sentence was an "acceptable" or "unacceptable" condition of the sentence (see Tyler et al., 2011, for details). An analysis of variance on the acceptability judgments (i.e., rating the sentences as acceptable or unacceptable) with age and ambiguity conditions as factors showed a strong main effect of condition ($F(2,122) = 98.59$; $p < 10^{-16}$). Post-hoc Tukey tests resulted in greater numbers of unacceptable judgments to subordinate compared with dominant sentences ($p < 10^{-7}$), to subordinate compared with unambiguous sentences ($p < 10^{-7}$), and no differences between dominant and unambiguous sentences ($p = 0.15$). There was no main effect of age ($F(1,122) = 1.24$; $p = 0.27$) and no interaction between age and condition ($F(2,122) = 0.16$; $p = 0.86$). Syntactic sensitivity (difference between rejection of subordinate and dominant sentences) also showed no effect of age (see Supplementary Fig. 3). These results are consistent with previous studies showing no overall age-related declines for syntactic processing (Tyler et al., 2010).

3.2. Global effects

3.2.1. Global GMD and age

We first correlated age and global GMD (averaged across the entire language network). Global GMD showed a significant negative correlation with age ($r = -0.756$; $t = -7.4$; $df = 41$; $p = 4.5 \times 10^{-9}$), consistent with previous findings (Sowell et al., 2003).

3.2.2. Differential effects of global GMD and age on global FCI

We then performed a linear regression on global FCI values (averaged across the entire language network) with the continuous variables of age and global GMD within the network as factors, to study their respective contributions to global FCI. Global GMD showed a significant main effect ($F(1,124) = 19.6$; $p = 2 \times 10^{-5}$) but chronological age was not significant ($F(1,124) = 2.34$; $p = 0.13$). There was no significant interaction between age and global GMD ($F(1,124) = 3.45$; $p = 0.07$). Global FCI and chronological age ($r = 0.057$; $t = 0.64$; $df = 127$; $p = 0.52$) were not significantly correlated. We found a significant negative correlation between global FCI and global GMD ($r = -0.28$; $t = -0.34$; $df = 127$; $p = 0.0011$). These results show that global functional connectivity is not directly influenced by chronological age, but increases strongly as global GMD decreases (Rabbitt et al., 2008).

To further determine the differential contributions of global GMD and age on global FCI we computed overlap correlations (Meng et al., 1992) between global FCI and global GMD and also between global FCI and age, taking into account the correlation between global GMD and age. Overlap correlations show the difference in the correlation between a main factor (in our case, global FCI) and two secondary factors (age and global GMD), considering that the secondary factors are correlated with each other. The results show a significant difference between the correlation of FCI and age, and the correlation of FCI and global GMD ($N = 129$; $z = 2.09$; $p = 0.036$), suggesting again that global GMD is the primary driver affecting global FCI.

3.2.3. Differential effects of global GMD and age on global efficiency

We next computed the integrated global efficiency, to assess how information transfer within the network changes with age and/or global GMD. We performed a linear regression on the integrated global efficiency values with the continuous variables of age and global GMD as factors, to study their respective contributions to network efficiency. We found a significant main effect of global GMD ($F(1,124) = 10.06$; $p = 0.002$), no significant main effect of age ($F(1,124) = 0.019$; $p = 0.89$), and no significant interaction between age and global GMD ($F(1,124) = 1 \times 10^{-5}$; $p = 0.99$). Network efficiency was significantly positively correlated with global GMD ($r = 0.19$; $t = 2.15$; $df = 127$; $p = 0.03$), but did not correlate with age ($r = -0.01$; $t = -0.13$; $df = 127$; $p = 0.89$). Network efficiency was also negatively correlated with global FCI ($r = -0.30$; $t = -3.64$; $df = 127$; $p = 0.0004$). Thus, network efficiency decreases as global FCI increases, and has the same dependence pattern as global FCI to global GMD and age. Thus, as GMD decreases with age, network organization changes so that there is increased, but less efficient, functional connectivity.

3.2.4. Influence of head motion on global variables

Recent studies (Power et al., 2012; Van Dijk et al., 2012) suggest that head motion might have an influence on functional connectivity results, in particular when assessing age differences. To confirm that our results are not the product of residual head motion, we computed the three parameters used by van Dijk et al. (2012), and examined their influence on the results. van Dijk et al. (2012) defined displacement as the mean-squared root of the translation in the three possible directions (x, y, z). The three movement parameters are then defined as (1) Mean motion: average of the displacement over the three sessions; (2) Max motion: maximum value of displacement achieved over the three sessions; and (3) Number of motions: the number of volumes in which a displacement is greater than 0.1 mm. Fig. 2 (top row) shows the correlations between the head movement parameters. As in van Dijk et al. (2012), the 3 parameters are strongly correlated: Mean motion versus Max motion ($r = 0.72$; $t = 6.7$; $df = 41$; $p = 4.4 \times 10^{-8}$; left panel), Mean motion versus Number of motions ($r = 0.75$; $t = 7.39$; $df = 41$; $p = 4.6 \times 10^{-9}$; middle panel), and Max motion versus Number of motions ($r = 0.49$; $t = 3.65$; $df = 41$; $p = 7.3 \times 10^{-4}$; right panel). Because the three movement parameters are strongly correlated, we selected mean head motion to examine the influence of head motion on the global variables previously computed, as in van Dijk et al. (2012). Fig. 2 (middle row) shows the correlations between the mean head motion and the global values: average GMD (left), age (middle), and average FCI (right). There was no significant correlation between head motion and age ($r = 0.05$; $t = 0.62$; $df = 41$; $p = 0.71$), or GMD ($r = -0.02$; $t = -0.13$; $df = 41$; $p = 0.89$). The influence is stronger on FCI, but still not significant ($r = -0.15$; $t = -1.81$; $df = 127$; $p = 0.07$). Head movements thus have a weak influence on the data. Considering these findings, we recomputed the correlations that we previously computed at the global level, with mean head motion regressed out (Fig. 2, lower row). We found that age and average GMD (left) were still strongly negatively correlated ($r = -0.75$; $t = -7.4$; $df = 41$; $p = 4.4 \times 10^{-9}$),
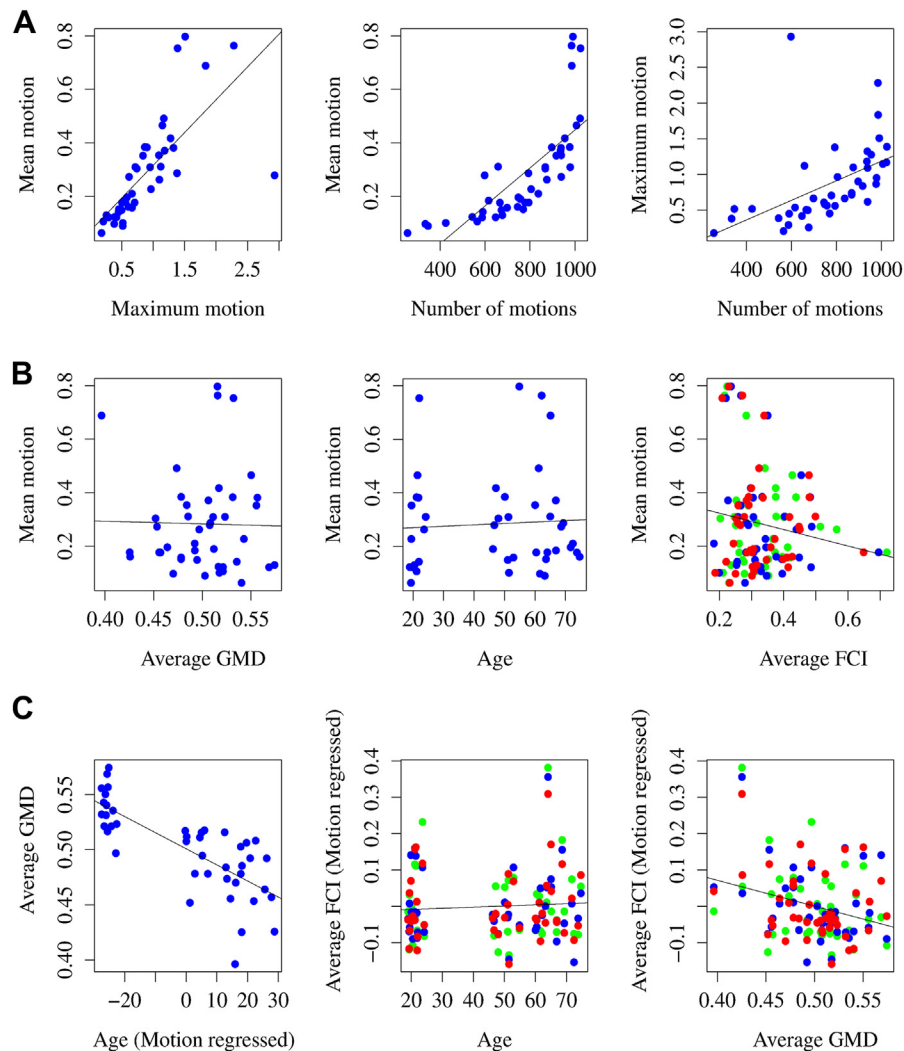
Fig. 2. Influence of head motion parameters on global parameter results. (A) Correlations between head motion parameters: mean motion and maximum motion (left), mean motion and number of motions (middle), and maximum motion and number of motions. (B) Correlations between mean head motion and global parameters: average GMD (left), age (middle), and average FCI (right). (C) Correlations between global parameters when mean head motion is regressed out: age and average GMD (left), age and average FCI (middle), and average FCI and average GMD (right). Abbreviations: FCI, functional connectivity index; GMD, gray matter density.

age was not correlated with average FCI ($r = 0.06$; $t = 0.76$; $df = 127$; $p = 0.45$), and average FCI was strongly negatively correlated with average GMD ($r = -0.29$; $t = -3.43$; $df = 127$; $p = 8.1 \times 10^{-4}$). Therefore, our findings hold when head movement is taken into account. The difference between our findings and those of van Dijk et al. (2012) might arise from that fact that theirs was a resting-state study whereas we computed network connectivity within a cognitive activation-related framework.

3.3. Regional effects of ROIs within the language template

3.3.1. Regional GMD and age

The results reported in the previous sections showed that global GMD and age are negatively correlated. Here we carried out a more detailed analysis of changes within the language system by examining the relationship between age and GMD in each of the 166 ROIs that comprise the network. In Fig. 3 are the correlations between GMD and age for each ROI. All the significant correlations between GMD and age (67 of 166 ROIs in total) were negative suggesting that regional decreases in GMD were associated with increasing age.

In Table 2, the number of ROIs in which there is a significant negative correlation with age are shown. This is also expressed as a

percentage of all ROIs in the AAL area of which they are part (e.g., percentage of ROIs within the LIFG that significantly correlated with age). We used this percentage as a measure of age-related GMD decline and found that the areas most sensitive to GMD decreases were the left IFG triangularis (64%) and bilateral IFG opercularis (left: 67%; right: 80%). The anterior parts of the temporal lobes (especially the bilateral superior temporal gyri—left: 57%; right: 47%) also suffered extensive GMD declines with age. In contrast, GMD was relatively preserved in bilateral MTG areas (left: 30%; right: 18%).

3.3.2. Effect of regional GMD on regional FCI

We next examined the relationship between regional GMD and regional FCI, by computing correlations between GMD in each ROI, and FCI between this ROI and all other ROIs in the language network. In Fig. 4, the results obtained for all ROIs are shown (top row: significant positive correlations; bottom row: significant negative correlations). The overall pattern shows that most of the significant correlations were negative (160 of 168), suggesting that age-related decreases in GMD are related to increasing regional FCI and this results in the overall reduction in network efficiency. We observed a diffuse pattern of negative correlations involving most
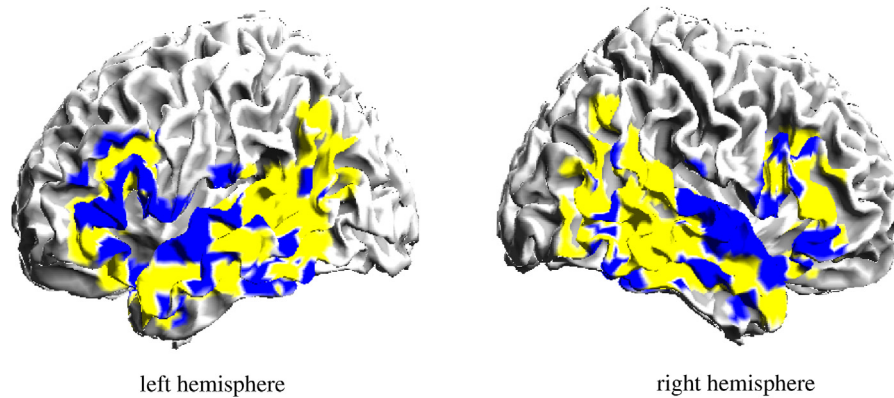
left hemisphere   right hemisphere

Fig. 3. Correlation between gray matter density (GMD) in each region of interest (ROI) and age. Blue indicates ROIs showing a negative correlation between age and GMD at the false discovery rate-corrected threshold. Yellow ROIs are regions included in the language template that show no significant correlation between GMD and age.

of the ROIs. Approximately half of these correlations are between interhemispheric ROIs (85 of 160), in particular between ROIs in left IFG opercularis and triangularis, and right ITG. Therefore, several bihemispheric pairs of ROIs show increases in FCI values with decreased GMD. Moreover, a few negative correlations between FCI and GMD are found between ROIs in the left IFG triangularis and orbalis.

Very few connections show a positive correlation with GMD (8 of 168), seven located mostly between ROIs within the left hemisphere and one between hemispheres, suggesting that reduced regional gray matter density is associated with decreased FCI in these areas.

Interestingly, there is a specific pattern of positive correlations for LIFG triangularis and LMTG, within and between these areas: only for ROIs within and between these two areas is reduced GMD associated with a decrease in FCI. These two areas are typically

Table 2
Number of ROIs showing a significant correlation between age and GMD within each AAL area

AAL area	Number of significant ROIs/total number of ROIs in AAL area	Percentage of significant ROIs
ORBinf.L	2/7	29
ORBinf.R	5/9	56
IFGtriang.L	9/14	64
IFGtriang.R	3/9	33
IFGoperc.L	2/3	67
IFGoperc.R	4/5	80
TPOsup.L	2/6	33
TPOsup.R	5/10	50
ITG.L	4/9	44
ITG.R	4/10	40
MTG.L	7/23	30
MTG.R	4/22	18
STG.L	8/14	57
STG.R	7/15	47
ANG.L	0/5	0
ANG.R	1/5	20

The first column shows number of significant ROIs/total number of ROIs in the specific AAL area, and the second column shows the same ratio, expressed as a percentage of significant ROIs within each AAL area.
Key: AAL, automated anatomical Labeling; ANG.L, left angular gyrus; ANG.R, right angular gyrus; GMD, gray matter density; IFGoperc.L, opercular part of the left inferior frontal gyrus; IFGoperc.R, opercular part of the right inferior frontal gyrus; IFGtriang.L, triangular part of the left inferior frontal gyrus; IFGtriang.R, triangular part of the right inferior frontal gyrus; ITG.L, left inferior temporal gyrus; ITG.R, right inferior temporal gyrus; MTG.L, left middle temporal gyrus; MTG.R, right middle temporal gyrus; ORBinf.L, orbital part of the left inferior frontal gyrus; ORBinf.R, orbital part of the right inferior frontal gyrus; ROI, region of interest; STG.L, left superior temporal gyrus; STG.R, right superior temporal gyrus; TPOsup.L, left superior temporal pole; TPOsup.R, right superior temporal pole.

activated in studies of language comprehension (Caplan, 1999; Hagoort, 2003; Tyler et al., 2010), and intact functional and anatomical connectivity between them is associated with intact performance (Griffiths et al., 2013; Papoutsi et al., 2011; Tyler and Marslen-Wilson, 2008).

Considering the importance of left frontotemporal connectivity for language function, we assessed relationships between GMD and FCI within and between ROIs in the LIFG triangularis and LMTG. The results indicate that these two areas might comprise functional subdivisions and additionally suggest some functional differentiation in the sensitivity within parts of the LIFG triangularis. Supplementary Fig. 4 shows patterns of positive and negative correlations for these two AAL areas suggesting that that the standard AAL areas used in connectivity and aging analyses might not provide sufficient spatial resolution to determine the detailed changes in patterns of connectivity with age.

3.3.3. Effect of age on regional FCI

Significant correlations between FCI for each pair of ROIs and age are shown in Fig. 5. In the correlations between FCI and age, we found 25 positive (Fig. 5, all panels, top row) and 32 negative correlations (Fig. 5, bottom row). The numbers of positive and negative correlations are relatively balanced across the hemispheres, but the sign of correlation differs across the hemispheres: FCI values tend be positive (greater with age) in the right hemisphere, and negative (weaker with age) in the left hemisphere. FCI values within the right MTG, and between the MTG/STG within and between hemispheres increase with age. In addition, there was increased bilateral connectivity primarily between the LMTG and the right IFG (RIFG) and right MTG. We also found that FCI decreased with age within the IFG triangularis in both hemispheres. Bilateral connections between ROIs in temporal areas increase with age, whereas connections within left and right IFG triangularis decrease with age.

3.3.4. Differential effects of GMD and age on regional FCI

To quantify the amount of variance in FCI that can be explained by each factor (chronological age and GMD), we used a general linear model for each FCI obtained for ROI pairs in the network and compared these values with the mean sum of squares (MSS) test (Supplementary Fig. 5). GMD explains most of the variance in the FCI datasets and the rest of the variance is explained by age. Because the two MSS distributions are not Gaussian (1-sample Kolmogorov-Smirnov normality test with similar mean and variance, for age: $D = 0.57$; $p < 2.2e\text{-}16$; and GMD: $D = 0.40$; $p < 2.2e\text{-}16$) and MSS values for age and GMD were obtained from the same general linear model, we used the Wilcoxon paired rank test to assess differences in MSS for GMD and age. The statistical test resulted in a highly significant
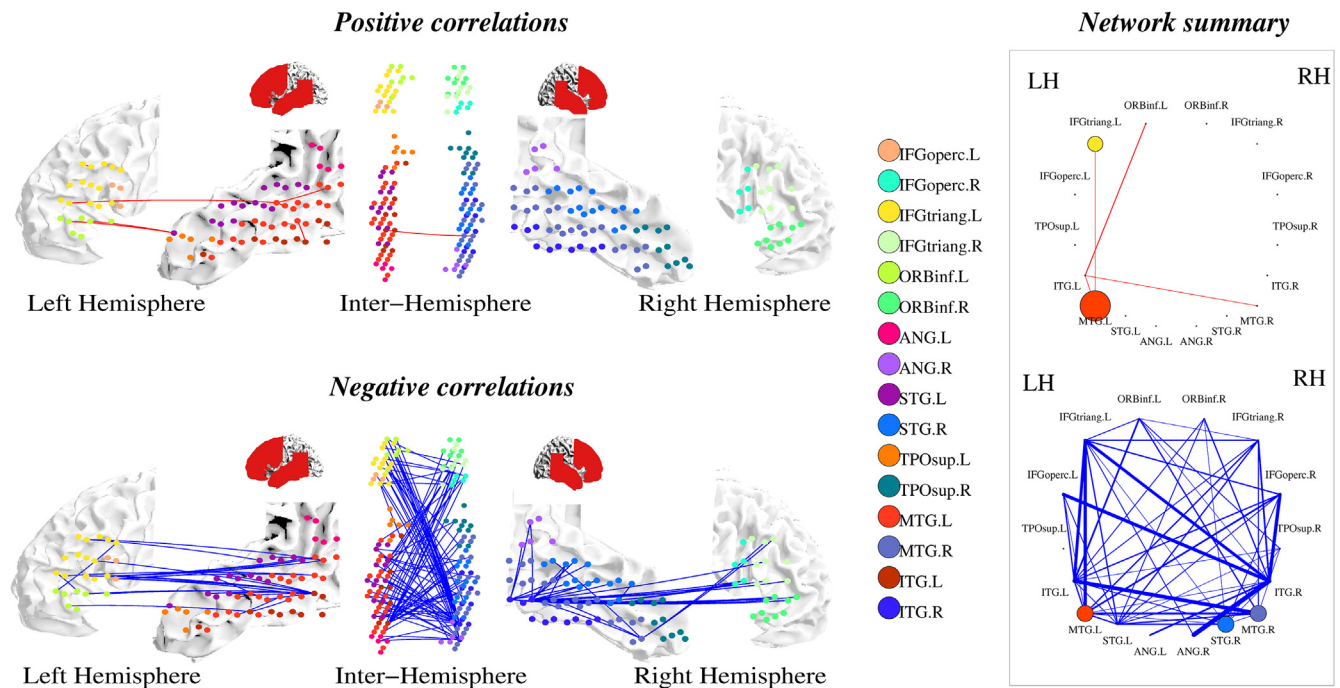
Fig. 4. Correlations between GMD in each region of interest (ROI) and functional connectivity index for each pair involving this ROI. Positive (top row, red for significance at the false discovery rate-corrected threshold) and negative (bottom row, blue for significance at the false discovery rate-corrected threshold) correlations between functional connectivity index and GMD are represented in separate panels. Figures in each panel correspond to significant correlations within the left hemisphere (viewed from the left side), between the 2 hemispheres (viewed from the top), and within the right hemisphere (viewed from the right side). On the right section of the figure there are summary representations of both networks, in which significant correlations are gathered according to Automated Anatomical Labeling (AAL) areas: edges between 2 nodes correspond to the number of significant correlations between ROIs in different AAL areas, and the size of the nodes corresponds to correlations between ROIs in the same AAL area. See Table 2 for abbreviations.

difference between the MSS for the 2 factors ($W = 44 \times 10^6$; $p < 10^{-16}$), thus showing that GMD explains more variance in the pairwise FCI datasets than does chronological age.

3.4. Relationship between regional FCI and performance

We next calculated the correlation between FCI values for each pair of ROIs in the network and syntactic sensitivity, assessed according to the differences in acceptability judgments between subordinate and dominant ambiguous sentences (see 2. Methods). In Fig. 6, FCI values are shown to be correlated negatively (in 15 pairs of ROIs) with syntactic sensitivity. No positive correlations were found. Most of these negative correlations were located within the right hemisphere (six correlations) and between hemispheres (seven correlations). The two negative correlations found within the left hemisphere involved the LMTG and the LIFG orbitalis. Thus, increased syntactic sensitivity (assessed according to behavioral performance) is associated with reduced connectivity (1) primarily between areas in the LMTG and LIFG orbitalis; (2) between several regions within the RH; and (3) between the LMTG and several regions in the RH. These findings suggest that there is increased connectivity between regions which are not essential for syntactic processing, without any decreased connectivity between the LMTG-LIFG triangularis, regions that are well established as being necessary for syntactic analysis.

4. Discussion

In this study we explored the relationship between age-related changes in local GMD and the network properties of the neural language system. We focused on language comprehension because it is typically preserved across the adult life span, and on syntax in

particular, because it is known to involve a strongly left-lateralized neural system. This study provided the opportunity to question whether and how the network structure underpinning syntax comprehension reorganizes in the face of widespread gray matter changes and whether the syntax network changes are related to functional changes within the wider language system, in the context of preserved function. To address these issues, we analyzed the network properties of fMRI data collected in an experiment in which participants across the adult life span listened to spoken sentences. We established in subsequent behavioral testing that there were no age-related changes in performance. The set of analyses we discuss here reveal the manner in which the network properties of the neural language system change within the context of preserved language function. The behavioral results show that aging did not affect participants' sensitivity to syntactic structure (Supplementary Fig. 3), consistent with previous data using different stimuli and tasks but addressing similar issues (Tyler et al., 2011).

An important aspect of our findings is that the differences in the relationship between GMD and functional connectivity cannot be attributed to age. This was evidenced by the very weak direct effect of age on functional connectivity. Although in general, GMD decreases with age, there is also considerable interparticipant variability in the amount of gray matter loss. Indeed, age-related variability in a variety of structural changes is a hallmark of healthy aging. There are several known influences on GMD such as physical (Kramer and Erickson, 2007; Rovio et al., 2010; Thomas et al., 2012) and intellectual activities (Anderton, 2002), some of which are known to interact with age in their effects on gray matter. If gray matter is preserved in older participants because of the effects of physical and intellectual activities, then FCI might reflect this.

Considering the effects of GMD and age on overall functional connectivity, we found that decreasing local GMD was associated
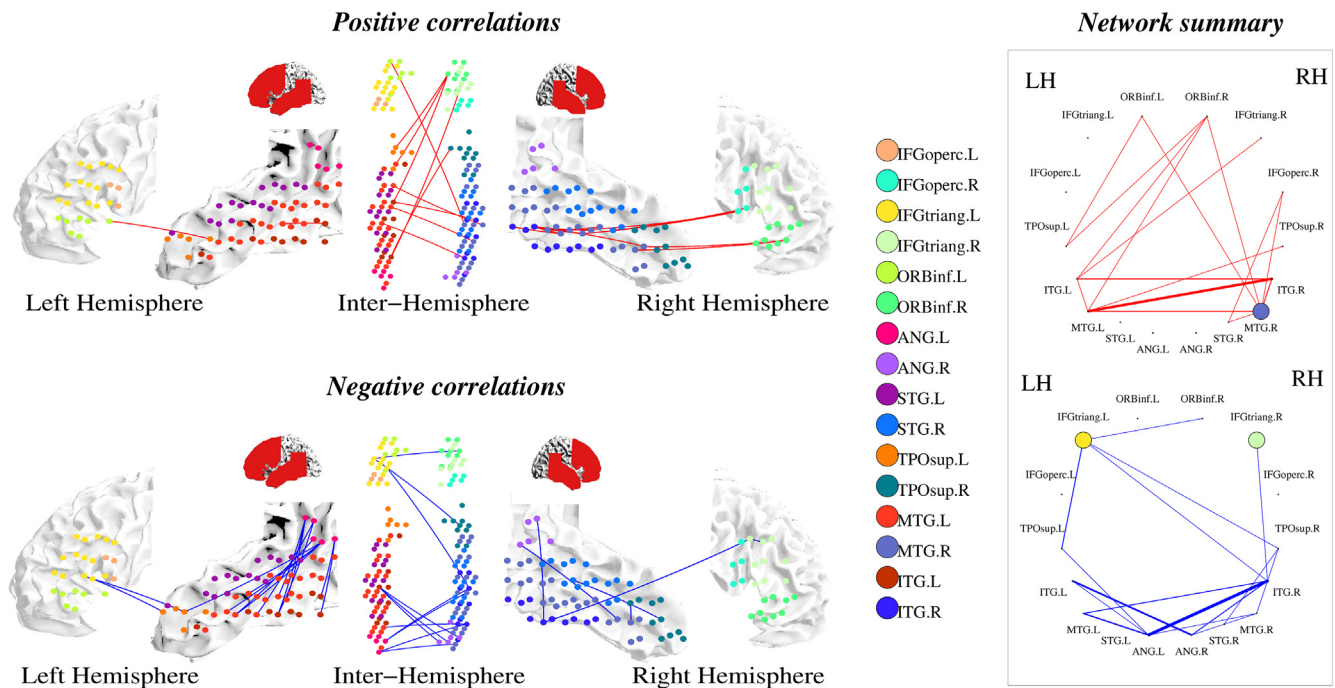
Fig. 5. Correlations between age and functional connectivity index for each pair of regions of interest (ROIs). Positive (top row, red for significance at the false discovery rate-corrected threshold) and negative (bottom row, blue for significance at the false discovery rate-corrected threshold) correlations between functional connectivity index and age are represented on separate panels. Figures in each panel correspond to significant correlations within the left hemisphere (viewed from the left side), between the 2 hemispheres (viewed from the top), and within the right hemisphere (viewed from the right side). On the right part of the figure are summary representations of both networks, in which significant correlations are gathered according to Automated Anatomical Labeling (AAL) areas: edges between 2 nodes correspond to the number of significant correlations between ROIs in different AAL areas, and the size of the nodes correspond to correlations between ROIs in the same AAL area. For the positive correlations, which indicate an increase in connectivity with increasing age, 13 were in the RH for both ROIs in the right hemisphere and 10 for ROIs in different hemispheres (2 for both ROIs in the left hemisphere), whereas for negative correlations, 15 were between ROIs in the left hemisphere, 6 for ROIs in the right hemisphere, and 11 for ROIs in different hemispheres. See Table 2 for abbreviations.

with changes in network connectivity such that connectivity within the RH increased and connectivity within the left hemisphere (LH) was reduced. The primary driver in the changes in functional connectivity was GMD rather than age. At the global level (for the entire language template), only GMD had an influence on FCI. Age and GMD had an effect at the regional FCI level, but even at this level GMD had a stronger influence than age (Supplementary Fig. 5). These findings support the claim that age-related changes in neurocognitive functions are caused by structural changes associated with age rather than by age itself (Park and Reuter-Lorenz, 2009). Moreover, these neuroanatomical changes had an effect on overall functional connectivity and network efficiency. Although functional connectivity increased with decreasing GMD, the efficiency of the network decreased.

Recent studies have revealed contradictory findings on the relative effect of age and gray matter on activation (Kalpouzos et al., 2012; Salami et al., 2012). Kalpouzos et al. (2012) showed that, for an episodic memory task, areas such as the enthorhinal cortex were activated differentially in young and older adults but the effect of age was very small when gray matter volumes were regressed out. In a very similar task, but using singular value decomposition over the whole brain, Salami et al. (2012) showed an effect of age on bilateral hippocampus activations, still present when gray matter volumes were regressed out. Although in our case, the effect of age and gray matter is discussed and analyzed in the context of FCI, some comparisons can be made: in the studies by Kalpouzos et al. (2012) and Salami et al. (2012), the effect of age and gray matter on activation is studied for a subset of areas showing an age-related effect. In our study we observed similar findings in the context of regional connectivity analyses (i.e., we also obtained some FCI values showing age-related effects as shown in Fig. 5). However,

when we consider average values over the whole system, the effect of age diminishes. Second, in activation studies, as stated for example, in Kalpouzos et al. (2012), some areas might show underactivation, and others show overactivation with age. When we examined the effect of age, the numbers of pairs showing positive and negative correlations with FCI were roughly equal, whereas, when we examined the effect of GMD, the number of negative correlations with FCI was much higher than the number of positive correlations. We must stress here that direct comparisons between the Kalpouzos and Salami studies and our study are difficult because theirs were activation studies and ours involved connectivity analyses.

With respect to network changes in frontal and temporal regions involved in syntax comprehension, decreasing GMD was associated with increasing connectivity within the LMTG and between MTG and STG within and between hemispheres, and with decreasing connectivity within LIFG regions (Brodmann area 45). Thus, as GMD decreases, the contribution of the LMTG increases in the context of decreased connectivity within the LIFG. Because frontal and parietal areas have been shown to suffer more GMD decreases with age than temporal areas (Good et al., 2001; Fig. 3 and Table 2), we hypothesize that the reorganization of the neural language system at the functional level might be underpinned by changes at the structural level, although our analysis cannot indicate the precise nature of the causal relationship between structural and functional factors. A more sensitive measure of network changes was provided by the correlation between GMD in each ROI and the functional connectivity values involving that ROI. Decreases in GMD were associated with increases and decreases in functional connectivity. Decreases in GMD were only associated with decreases in functional connectivity between and within ROIs
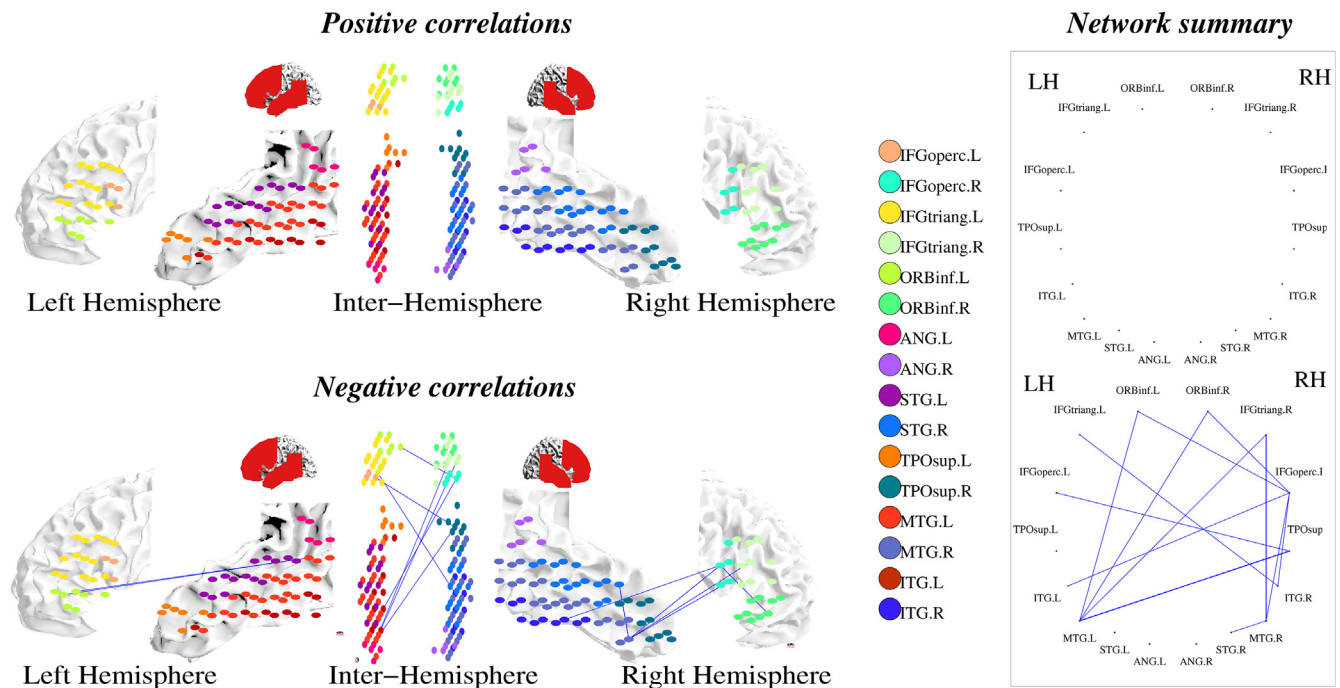
Fig. 6. Correlation between syntactic sensitivity measure (subordinate−dominant rejection rates) and functional connectivity values for each pair of regions of interest (ROIs). Positive (top row, red for significance at the false discovery rate-corrected threshold) and negative (bottom row, blue for significance at the false discovery rate-corrected threshold) correlations with gray matter density are represented on separated panels. Figures in each panel correspond to significant correlations within the left hemisphere (viewed from the left side), between the 2 hemispheres (viewed from the top), and within the right hemisphere (viewed from the right side). On the right part of the figure are summary representations of both networks, in which significant correlations are gathered according to Automated Anatomical Labeling (AAL) areas: edges between 2 nodes correspond to the number of significant correlations between ROIs in different AAL areas, and the size of the nodes corresponds to correlations between ROIs in the same AAL area. See Table 2 for abbreviations.

in the LIFG (Brodmann area 45) and LMTG (Fig. 3). However, different ROI subdivisions within the LIFG and the LMTG were involved in increased connectivity within and across hemispheres, and this in turn was associated with decreased local GMD.

One of the main interests prompting this research concerned the relationship between functional connectivity within the syntax network and its relationship with the wider language network, in the context of GMD changes with age and preserved syntax. The graph analyses results showed that decreases in GMD produced an overall increase in FCI across the whole language template. However, in contrast, the functional system involved in syntax processing (within and between ROIs in the LIFG and LMTG) showed decreased connectivity as GMD decreased. This finding, that positive correlations with GMD were only associated with FCI involving pairs of ROIs with one node in the left IFG triangularis and the other in left MTG, provides a possible explanation for the origin of age-related functional network reorganization; namely, that decreased connectivity within the syntax network might trigger increased connectivity throughout the wider language system. Moreover, the fact that we find increases in functional connectivity across the whole network, in the context of reduced functional connectivity between areas known to be involved in the syntax network and preserved function, supports the hypothesis that aging is associated with a loss of specific functional connections in favor of a more diffuse network, known as the dedifferentiation hypothesis (de Frias et al., 2007; Grady et al., 1999). Importantly, our results suggest that dedifferentiation is related most strongly to structural brain changes rather than to age per se. We have shown, using a Wilcoxon paired rank test on the MSS values obtained for each pair of ROIs in the network, that the observed functional reorganization is primarily associated with local GMD, and only secondarily with age. Thus, a measure of neuroanatomic variations

appears to be a better predictor than age for studying the origin of the age-related differences observed in functional networks.

These results are relevant to the issue of compensatory processes in aging. However, they are not consistent with the HAROLD model in which increases in contralateral activity are associated with preserved cognition in aging. In our data, we found that RH increases in FCI were associated with lower acceptability scores to subordinate sentences, a behavioral pattern which is associated with syntactic impairment (see Tyler et al., 2011). We observed similar results in a previous study on language processing which showed age-related decreases in the integrity of the LIFG accompanied by increased functional activity in the RIFG (Tyler et al., 2010), but without any improvement in language function. These data are best accounted for by a theoretical model of aging that claims that less specialized activity in the nondominant hemisphere might have adverse effects for cognition (e.g., Persson et al., 2006).

In the present study, functional connectivity involving the RIFG increased as part of the changes in connectivity involving the wider language network, and not as part of the syntax network. Here we also found only negative correlations between pairwise FCI and syntactic sensitivity, and these only involved connections between areas that are not normally associated with syntactic processing: areas within the RH, between areas in the LIFG and RH, and between the LMTG and areas in the RH. Considering that the functional system supporting syntactic processing primarily involves connectivity between the LIFG triangularis and LMTG (Griffiths et al., 2013; Tyler et al., 2011), we found: (1) stronger FCI values between core language areas in the LH and areas located in the contralateral hemisphere (increased FCI values between the LMTG and several areas in the RH, and between the LIFG orbitalis and several areas in the RH); and (2) recruitment of areas located close to the core language areas (increased FCI values between the LMTG

and LIFG orbitalis, the latter being contiguous to the LIFG triangularis). Overall, this recruitment of new areas is associated with a decrease in syntactic sensitivity, suggesting that it does not serve to preserve cognitive function.

We also found that the increase in FCI is related to a decrease in efficiency; a smaller, more specialized system is more efficient than a diffuse system. van den Heuvel et al. (2009) suggested that network efficiency in the resting state was associated with intellectual performance. This model is consistent with the reduction of efficiency associated with GMD we observed here, because reduced gray matter integrity led to the recruitment of new areas. This more extensive system includes areas that do not perform the same function but rather support the functionality of the residue of the core system whose effectiveness has been reduced with gray matter changes (as is the case for the LIFG triangularis).

In this study we have focused only on age-related changes in gray matter integrity and how they relate to changes in functional connectivity. However, although there is indisputable evidence that white matter tracts also change with age (Abe et al., 2002; Head et al., 2004; Madden et al., 2004; Salat et al., 2005; Stamatakis et al., 2011), the role of white matter changes and their relationship to changes in functional connectivity was beyond the scope of our investigation. Nonetheless, it is notable that graph theoretical investigations of white matter connectivity in normal young adults (Hagmann et al., 2008) and older adults (Gong et al., 2009) reveal a substantial overlap in the interregional covariance between gray and white matter (Gong et al., 2013), suggesting that the observed effect in our analysis might also be observed in comparable analyses on the white matter tracts.

As a methodological note, we have also shown that our findings are robust regardless of whether head motion is taken into account. Head motion has been shown to influence the results in resting-state connectivity studies but this is not the case in the cognitive activation fMRI data we present herein (Fig. 2). We have also shown that the results do not change significantly with the type of band-pass filtering used at the preprocessing stage and because there is no consensus on the type of filtering to use when investigating complex cognitive networks, we included summary results obtained for different kinds of filtering (Supplementary Figs. 6 and 7). Finally, we addressed the issue of the contribution of possible outliers in the overall pattern of findings by showing that correlations obtained between average FCI, age, and average GMD were not because of the presence of outliers (Supplementary Fig. 8).

Another methodological note is on our use of unmodulated gray matter segmented images because there is some debate as to whether it is preferable to use modulated or unmodulated images. For completeness we provide data from modulated gray matter segments in the Supplementary data (see Supplementary Fig. 2). The correlation between modulated and unmodulated values is highly significant: (1) for all ROIs in all participants: ($r = 0.832$; $t = 129$; $df = 7136$; $p < 10^{-15}$); and (2) more importantly, for our analysis between ROIs for gray matter values averaged over participants ($r = 0.909$; $t = 27.9$; $df = 164$; $p < 10^{-15}$). However, modulated values are overall lower than unmodulated values (mean modulated: 0.38; mean unmodulated: 0.50), and a paired t test over all ROIs in all participants resulted in a significant effect ($t = -114$; $df = 7137$; $p < 10^{-15}$). Nevertheless, the highly significant correlation between modulated and unmodulated values suggests that if we had used modulated values instead in our analyses, the results would have been similar.

In sum, this research provides a method for analyzing cognitive activation-related fMRI data within the framework of complex networks. We have illustrated a method for defining functional networks at the single-participant level for each experimental condition, and related their properties to demographic, anatomic, and behavioral measurements. We applied this method to syntax comprehension, a cognitive process shown to be strongly lateralized, to test different hypotheses regarding aging and reorganization of functional networks. We provide suggestions on the origin of the observed differences in functional connectivity across the adult life span, because these differences are primarily related to GMD, and only secondarily to aging.

Disclosure statement

None of the authors have any conflicts of interest to disclose.

All procedures involving human participants were reviewed and approved by the East of England - Essex (formerly Suffolk) Research Ethics Committee before participant participation.

Appendix A. Supplementary data

Supplementary data associated with this article can be found, in the online version, at http://dx.doi.org/10.1016/j.neurobiolaging.2013.07.003.

References

Abe, O., Aoki, S., Hayashi, N., Yamada, H., Kunimatsu, A., Mori, H., Yoshikawa, T., Okubo, T., Ohtomo, K., 2002. Normal aging in the central nervous system: quantitative MR diffusion-tensor analysis. Neurobiol. Aging 23, 433—441.
Achard, S., Bullmore, E., 2007. Efficiency and cost of economical brain functional networks. PLoS Comput. Biol. 3, e17.
Anderton, B.H., 2002. Ageing of the brain. Mech Ageing Dev. 123, 811—817.
Ashburner, J., Friston, K.J., 2005. Unified segmentation. Neuroimage 26, 839—851.
Bassett, D.S., Wymbs, N.F., Porter, M.A., Mucha, P.J., Carlson, J.M., Grafton, S.T., 2011. Dynamic reconfiguration of human brain networks during learning. Proc. Natl. Acad. Sci. U.S.A 108, 7641—7646.
Bozic, M., Tyler, L.K., Ives, D.T., Randall, B., Marslen-Wilson, W.D., 2010. Bihemispheric foundations for human speech comprehension. Proc. Natl. Acad. Sci. U.S.A. 107, 17439—17444.
Bright, P., Moss, H.E., Stamatakis, E.A., Tyler, L.K., 2008. Longitudinal studies of semantic dementia: the relationship between structural and functional changes over time. Neuropsychologia 46, 2177—2188.
Buckner, R.L., Sepulcre, J., Talukdar, T., Krienen, F.M., Liu, H., Hedden, T., Andrews-Hanna, J.R., Sperling, R.A., Johnson, K.A., 2009. Cortical hubs revealed by intrinsic functional connectivity: mapping, assessment of stability, and relation to Alzheimer's disease. J. Neurosci. 29, 1860—1873.
Bullmore, E., Sporns, O., 2009. Complex brain networks: graph theoretical analysis of structural and functional systems. Nat. Rev. Neurosci. 10, 186—198.
Burke, D.M., Shafto, M.A., 2008. Language and aging. In: Craik, F.I., Salthouse, T.A. (Eds.), The Handbook of Aging and Cognition. Psychology Press, New York and Hove, pp. 373—443.
Burock, M.A., Buckner, R.L., Woldorff, M.G., Rosen, B.R., Dale, A.M., 1998. Randomized event-related experimental designs allow for extremely rapid presentation rates using functional MRI. Neuroreport 9, 3735—3739.
Cabeza, R., 2002. Hemispheric asymmetry reduction in older adults: the HAROLD Model. Psychol. Aging 17, 85—100.
Cabeza, R., Anderson, N.D., Locantore, J.K., McIntosh, A.R., 2002. Aging gracefully: compensatory brain activity in high-performing older adults. Neuroimage 17, 1394—1402.
Caplan, D., 1999. Activating brain systems for syntax and semantics. Neuron 24, 292—293.
Craik, F.I., Salthouse, T.A., 2000. The Handbook of Aging and Cognition. Lawrence Erlbaum Associates, Hillsdale, NJ.
Crinion, J.T., Lambon-Ralph, M.A., Warburton, E.A., Howard, D., Wise, R.J., 2003. Temporal lobe regions engaged during normal speech comprehension. Brain 126, 1193—1201.

Davis, S.W., Dennis, N.A., Buchler, N.G., White, L.E., Madden, D.J., Cabeza, R., 2009. Assessing the effects of age on long white matter tracts using diffusion tensor tractography. Neuroimage 46, 530–541.

Davis, S.W., Dennis, N.A., Daselaar, S.M., Fleck, M.S., Cabaza, R., 2008. Que PASA? The posterior-anterior shift in aging. Cereb. Cortex 18, 1201–1209.

Davis, S.W., Kragel, J.E., Madden, D.J., Cabeza, R., 2012. The architecture of cross-hemispheric communication in the aging brain: linking behavior to functional and structural connectivity. Cereb. Cortex 22, 232–242.

de Frias, C.M., Lovden, M., Lindenberger, U., Nilsson, L.G., 2007. Revisiting the dedifferentiation hypothesis with longitudinal multi-cohort data. Intelligence 35, 381–392.

Dodel, S., Golestani, N., Pallier, C., ElKouby, V., Le Bihan, D., Poline, J.B., 2005. Condition-dependent functional connectivity: syntax networks in bilinguals. Philos. Trans. R. Soc. Lond. B Biol. Sci. 360, 921–935.

Dronkers, N.F., Wilkins, D.P., Van Valin Jr, R.D., Redfern, B.B., Jaeger, J.J., 2004. Lesion analysis of the brain areas involved in language comprehension. Cognition 92, 145–177.

Eguiluz, V.M., Chialvo, D.R., Cecchi, G.A., Baliki, M., Apkarian, A.V., 2005. Scale-free brain functional networks. Phys. Rev. Lett. 94, 018102.

Ferreira, L.K., Busatto, G.F., 2013. Resting-state functional connectivity in normal brain aging. Neurosci. Biobehav. Rev. 37, 384–400.

Fornito, A., Zalesky, A., Bullmore, E.T., 2010. Network scaling effects in graph analytic studies of human resting-state fMRI data. Front. Sys. Neurosci. 4, 22.

Friston, K.J., Buechel, C., Fink, G.R., Morris, J., Rolls, E., Dolan, R.J., 1997. Psychophysiological and modulatory interactions in neuroimaging. Neuroimage 6, 218–229.

Ghisletta, P., Lindenberger, U., 2003. Age-based structural dynamics between perceptual speed and knowledge in the Berlin Aging Study: direct evidence for ability dedifferentiation in old age. Psychol. Aging 18, 696–713.

Ginestet, C.E., Nichols, T.E., Bullmore, E.T., Simmons, A., 2011. Brain network analysis: separating cost from topology using cost-integration. PLoS One 6, e21570.

Ginestet, C.E., Simmons, A., 2011. Statistical parametric network analysis of functional connectivity dynamics during a working memory task. Neuroimage 55, 688–704.

Gong, G., Rosa-Neto, P., Carbonell, F., Chen, Z.J., He, Y., Evans, A.C., 2009. Age- and gender-related differences in the cortical anatomical network. J. Neurosci. 29, 15684–15693.

Gong, N.J., Wong, C.S., Chan, C.C., Leung, L.M., Chu, Y.C., 2013. Correlations between microstructural alterations and severity of cognitive deficiency in Alzheimer's disease and mild cognitive impairment: a diffusional kurtosis imaging study. Magn. Reson. Imaging 31, 688–694.

Good, C.D., Johnsrude, I., Ashburner, J., Henson, R.N.A., Friston, K.J., Frackowiak, R.S., 2001. A voxel-based morphometric study of ageing in 465 normal adult human brains. Neuroimage 14, 21–36.

Grady, C.L., McIntosh, A.R., Rajah, M.N., Beig, S., Craik, F.I., 1999. The effects of age on the neural correlates of episodic encoding. Cereb. Cortex 9, 805–814.

Griffiths, J.D., Marslen-Wilson, W.D., Stamatakis, E.A., Tyler, L.K., 2013. Functional organization of the neural language system: dorsal and ventral pathways are critical for syntax. Cereb. Cortex 23, 139–147.

Hagmann, P., Cammoun, L., Gigandet, X., Meuli, R., Honey, C.J., Wedeen, V.J., Sporns, O., 2008. Mapping the structural core of human cerebral cortex. PLoS Biol. 6, e159.

Hagoort, P., 2003. How the brain solves the binding problem for language: a neurocomputational model of syntactic processing. Neuroimage 20 (suppl 1), S18–S29.

He, Y., Evans, A., 2010. Graph theoretical modeling of brain connectivity. Curr. Opin. Neurol. 23, 341–350.

Head, D., Buckner, R.L., Shimony, J.S., Williams, L.E., Akbudak, E., Conturo, T.E., McAvoy, M., Morris, J.C., Snyder, A.Z., 2004. Differential vulnerability of anterior white matter in nondemented aging with minimal acceleration in dementia of the Alzheimer type: evidence from diffusion tensor imaging. Cereb. Cortex 14, 410–423.

Hochberg, Y., 1988. A sharper Bonferroni procedure for multiple tests of significance. Biometrika 75, 800–802.

Indefrey, P., Cutler, A., 2004. Pre-lexical and lexical processing in listening. In: Gazzaniga, M.S. (Ed.), The Cognitive Neurosciences. MIT Press, Cambridge, MA, pp. 759–774.

Josephs, O., Henson, R.N., 1999. Event-related functional magnetic resonance imaging: modelling, inference and optimization. Philos. Trans. Roy. Soc. Lond. B Biol. Sci. 354, 1215–1228.

Kalpouzos, G., Persson, J., Nyberg, L., 2012. Local brain atrophy accounts for functional activity differences in normal aging. Neurobiol. Aging 33, 623 e1-623.e13.

Kramer, A.F., Erickson, K.I., 2007. Capitalizing on cortical plasticity: influence of physical activity on cognition and brain function. Trends Cogn. Sci. 11, 342–348.

Latora, V., Marchiori, M., 2001. Efficient behavior of small-world networks. Phys. Rev. Lett. 87, 198701.

Latora, V., Marchiori, M., 2003. Economic small-world behavior in weighted networks. Eur. Phys. J. B 32, 249–263.

Madden, D.J., Whiting, W.L., Huettel, S.A., White, L.E., MacFall, J.R., Provenzale, J.M., 2004. Diffusion tensor imaging of adult age differences in cerebral white matter: relation to response time. Neuroimage 21, 1174–1181.

Meier, T.B., Desphande, A.S., Vergun, S., Nair, V.A., Song, J., Biswal, B.B., Meyerand, M.E., Birn, R.M., Prabhakaran, V., 2012. Support vector machine classification and characterization of age-related reorganization of functional brain networks. Neuroimage 60, 601–613.

Meng, X.L., Rosenthal, R., Rubin, D.B., 1992. Comparing correlated correlation coefficients. Psychol. Bull. 111, 172–175.

Meunier, D., Achard, S., Morcom, A., Bullmore, E., 2009. Age-related changes in modular organization of human brain functional networks. Neuroimage 44, 715–723.

Newman, M.E., 2003. The structure and function of complex networks. SIAM Rev. 45, 167–256.

Papoutsi, M., Stamatakis, E.A., Griffiths, J.D., Marslen-Wilson, W.D., Tyler, L.K., 2011. Is left fronto-temporal connectivity essential for syntax? Effective connectivity, tractography and performance in left-hemisphere damaged patients. Neuroimage 58, 656–664.

Park, D.C., Polk, T.A., Park, R., Minear, M., Savage, A., Smith, M.R., 2004. Aging reduces neural specialisation in ventral visual cortex. Proc. Natl. Acad. Sci. U.S.A 101, 13091–13095.

Park, D.C., Reuter-Lorenz, P.A., 2009. The adaptive brain: aging and neurocognitive scaffolding. Annu. Rev. Psychol. 60, 173–196.

Persson, J., Nyberg, L., Lind, J., Larsson, A., Nilsson, L.G., Ingvar, M., Buckner, R.L., 2006. Structure-function correlates of cognitive decline in aging. Cereb. Cortex 16, 907–915.

Pfefferbaum, A., Sullivan, E.V., Hedehus, M., Lim, K.O., Adalsteinsson, E., Moseley, M., 2000. Age-related decline in brain white matter anisotropy measured with spatially corrected echo-planar diffusion tensor imaging. Magn. Reson. Med. 44, 259–268.

Power, J.D., Barnes, K.A., Snyder, A.Z., Schlaggar, B.L., Petersen, S.E., 2012. Spurious but systematic correlations in functional connectivity MRI networks arise from subject motion. Neuroimage 59, 2142–2154.

Price, C.J., 2012. A review and synthesis of the first 20 years of PET and fMRI studies of heard speech, spoken language and reading. Neuroimage 62, 816–847.

Rabbitt, P., Ibrahim, S., Lunn, M., Scott, M., Thacker, N., Hutchinson, C., Horan, M., Pendleton, N., Jackson, A., 2008. Age-associated losses of brain volume predict longitudinal cognitive declines over 8 to 20 years. Neuropsychology 22, 3–9.

Raven, J.C., 1995. Colored Progressive Matrices. Oxford Psychologists Press Ltd., Oxford.

Raz, N., Lindenberger, U., Rodrigue, K.M., Kennedy, K.M., Head, D., Williamson, A., Dahle, C., Gerstorf, D., Acker, J.D., 2005. Regional brain changes in aging healthy adults: general trends, individual differences and modifiers. Cereb. Cortex 15, 1676–1689.

Rovio, S., Spulber, G., Nieminen, L.J., Niskanen, E., Winblad, B., Tuomilehto, J., Nissinen, A., Soininen, H., Kivipelto, M., 2010. The effect of midlife physical activity on structural brain changes in the elderly. Neurobiol. Aging 31, 1927–1936.

Salami, A., Eriksson, J., Nyberg, L., 2012. Opposing effects of aging on large-scale brain systems for memory encoding and cognitive control. J. Neurosci. 32, 10749–10757.

Salat, D.H., Tuch, D.S., Greve, D.N., van der Kouwe, A.J., Hevelone, N.D., Zaleta, A.K., Rosen, B.R., Fischl, B., Corkin, S., Rosas, H.D., Dale, A.M., 2005. Age-related alterations in white matter microstructure measured by diffusion tensor imaging. Neurobiol. Aging 26, 1215–1227.

Salthouse, T.A., 1991. Theoretical Perspectives on Cognitive Aging. Lawrence Erlbaum Associates, Hillsdale, NJ.

Scott, S.K., Blank, C.C., Rosen, S., Wise, R.J., 2000. Identification of a pathway for intelligble speech in the left temporal lobe. Brain 123, 2400–2406.

Shinkareva, S.V., Mason, R.A., Malave, V.L., Wang, W., Mitchell, T.M., Just, M.A., 2008. Using fMRI brain activation to identify cognitive states associated with perception of tools and dwellings. PLoS One 3, e1394.

Sowell, E.R., Peterson, B.S., Thompson, P.M., Welcome, S.E., Henkenius, A.L., Toga, A.W., 2003. Mapping cortical change across the human life span. Nat. Neurosci. 6, 309–315.

Stamatakis, E.A., Shafto, M.A., Williams, G., Tam, P., Tyler, L.K., 2011. White matter changes and word finding failures with increasing age. PLoS One 6, e14496.

Steiger, J.H., 1980. Tests for comparing elements of a correlation matrix. Psychol. Bull. 87, 245–251.

Taylor, K.I., Stamatakis, E.A., Tyler, L.K., 2009. Crossmodal integration of object features: voxel-based correlations in brain-damaged patients. Brain 132, 671–683.

Thomas, A.G., Dennis, A., Bandettini, P.A., Johansen-Berg, H., 2012. The effects of aerobic activity on brain structure. Front. Psychol. 3, 86.

Tomasi, D., Volkow, N.D., 2012. Aging and functional brain networks. Mol. Psychiatry 17, 471, 549–558.

Tyler, L.K., Marslen-Wilson, W.D., 2008. Fronto-temporal brain systems supporting spoken language comprehension. Philos. Trans. Roy. Soc. Lond. B Biol. Sci. 363, 1037–1054.

Tyler, L.K., Marslen-Wilson, W.D., Randall, B., Wright, P., Devereux, B.J., Zhuang, J., Papoutsi, M., Stamatakis, E.A., 2011. Left inferior frontal cortex and syntax: function, structure and behaviour in patients with left hemisphere damage. Brain 134, 415–431.

Tyler, L.K., Marslen-Wilson, W.D., Stamatakis, E.A., 2005. Dissociating neurocognitive component processes: voxel-based correlational methodology. Neuropsychologia 43, 771–778.

Tyler, L.K., Shafto, M.A., Randall, B., Wright, P., Marslen-Wilson, W.D., Stamatakis, E.A., 2010. Preserving syntactic processing across the adult life span: the modulation of the frontotemporal language system in the context of age-related atrophy. Cereb. Cortex 20, 352–364.

Tzourio-Mazoyer, N., Landeau, B., Papathanassiou, D., Crivello, F., Etard, O., Delcroix, N., Mazoyer, B., Joliot, M., 2002. Automated anatomical labeling of

activations in SPM using a macroscopic anatomical parcellation of the MNI MRI single-subject brain. Neuroimage 15, 273–289.

van den Heuvel, M.P., Stam, C.J., Kahn, R.S., Hulshoff, H.E., 2009. Efficiency of functional brain networks and intellectual performance. J. Neurosci. 29, 7619–7624.

van Dijk, K.R., Sabuncu, M.R., Buckner, R.L., 2012. The influence of head motion on intrinsic functional connectivity MRI. Neuroimage 59, 431–438.

Vannest, J.J., Karunanayaka, P.R., Altaye, M., Schmithorst, V.J., Plante, E.M., Eaton, K.J., Rasmussen, J.M., Holland, S.K., 2009. Comparison of fMRI data from passive listening and active-response story processing tasks in children. J. Magn. Reson. Imaging 29, 971–976.

Wang, J., Zuo, X., He, Y., 2010. Graph-based network analysis of resting-state functional MRI. Front. Syst. Neurosci. 4, 16.

Wang, L., Li, Y., Metzak, P., He, Y., Woodward, T.S., 2012. Age-related changes in topological patterns of large-scale brain functional networks during memory encoding and recognition. Neuroimage 50, 862–872.

Yang, Y., Liang, P., Lu, S., Li, K., Zhong, N., 2009. The role of the DLPFC in inductive reasoning of MCI patients and normal agings: an fMRI study. Sci. China C Life Sci. 52, 789–795.

Zalesky, A., Fornito, A., Harding, I.H., Cocchi, L., Yucel, M., Pantelis, C., Bullmore, E.T., 2010. Whole-brain anatomical networks: does the choice of nodes matter? Neuroimage 50, 970–983.